

Diffusion of alcohol-rhodamine 6G in polymethyl methacrylate

JUN'ICHIRO MUTO*, SHIGEKI TAJIKA†

Department of Instrumentation Engineering, Faculty of Science and Technology, Keio University, 3-14-1, Hiyoshi, Kohoku 223 Japan

Rhodamine 6G (Rh6G) is impregnated in polymethyl methacrylate by concentration difference diffusion method. The diffusion behaviour of ethanoic and methanoic Rh6G in polymethyl methacrylate at temperatures between 35 and 70°C were studied. The following results were obtained: (a) Visually observed sharp boundary, characteristic of Case II transport, during diffusion of alcohol penetrates at a rate of $1.7 \times 10^{-6} \text{ cm sec}^{-1}$ with an activation energy of 23 kcal mol^{-1} for ethanol-polymethyl methacrylate system and $1.0 \times 10^{-5} \text{ cm sec}^{-1}$, with 23 kcal mol^{-1} for methanol-polymethyl methacrylate, respectively, at 60°C. (b) Diffusion of alcoholic Rh6G in polymethyl methacrylate is greatly hindered since internal stresses exist in the swollen region of the glassy polymer. (c) Diffusion of alcoholic Rh6G in swollen polymethyl methacrylate with equilibrium alcohol concentration followed Fickian kinetics. The diffusion coefficient of Rh6G at 60°C is determined as $5.2 \times 10^{-8} \text{ cm}^2 \text{ sec}^{-1}$ with an activation energy of 41 kcal mol^{-1} for the wet ethanol-polymethyl methacrylate and $6.1 \times 10^{-8} \text{ cm}^2 \text{ sec}^{-1}$, with 34 kcal mol^{-1} for the wet methanol-polymethyl methacrylate systems, respectively.

1. Introduction

The diffusion processes of organic solvents in glassy polymers is discussed in terms of combination of Fickian and Case II mechanisms [1, 2]. Characteristic features of Case II transport are expressed as follows [3]:

(a) sharp boundary separates outer swollen rubber shell from inner glass core;

(b) the front mentioned in (a) advances with a constant velocity and the weight gain of penetrant at time (t) is proportional to t .

Generalized equation for diffusion in one dimension which embodies both Fickian and Case II contributions is expressed as [3, 4]

$$\frac{\partial C}{\partial t} = \frac{\partial}{\partial x} \left(D \frac{\partial C}{\partial x} - vC \right) \quad (1)$$

where C is the concentration of the diffusant at x ; D is the diffusion coefficient; v is the velocity of Case II transport, and t represents time. The first term in the bracket shows Fickian diffusion, and the second, Case II transport. Case II diffusion in glassy polymers is considered to be controlled by the mechanical response of the glass just ahead of the sharp front to an osmotic swelling stress [3].

Studies of the transport kinetics of liquid methanol in polymethyl methacrylate (PMMA) at temperatures between 62 and 0°C have revealed that at ambient temperatures and below, the diffusion behaviour is typical of Case II transport, but as the temperature is raised the diffusion process becomes significantly

Fickian in character [5]. The phenomena that were observed in the methanol-PMMA system, such as the anisotropic dimension changes of the sample, the effect of constraint on equilibrium absorption in swelling surface layers, the development of birefringence and the craze formation on desorption, are all the result of internal stresses generated during swelling and sorption processes [6].

Rhodamine 6G (Rh6G), the most widely used laser dye material belonging to the xanthene family, has succeeded to lase in the solid polymeric matrix of PMMA [7]. Introduction of xanthene dyes in polymeric substances can occur either by a concentration difference diffusion process or by solution polymerization.

A photobleaching study on Rh6G/PMMA at room temperature showed that the photofading quantum yield of Rh6G molecules doped by a concentration difference diffusion method was lower than that by solution polymerization under visible and u.v. irradiation [8]. Rh6G molecules are diffused in PMMA by immersing the polymer sample in either ethanoic or methanoic Rh6G solution. The diffusion behaviour of Rh6G, however, has not been clarified as yet. In this article, we have examined the transport properties of ethanoic and methanoic Rh6G in PMMA at temperatures between 35 and 70°C.

2. Experimental details

The PMMA sample was made as follows: the methylmethacrylate was vacuum distilled before polymerization. The polymerization catalyst was

*To whom all correspondence should be addressed.

†Present address: Mitsui Trading Co. Ltd., 1-2-1, Ohtemachi, Chiyoda, Tokyo 100, Japan.

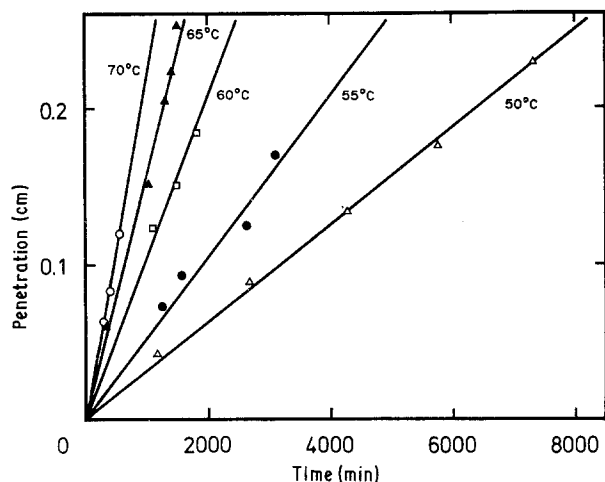


Figure 1 Penetration against time for ethanol in PMMA.

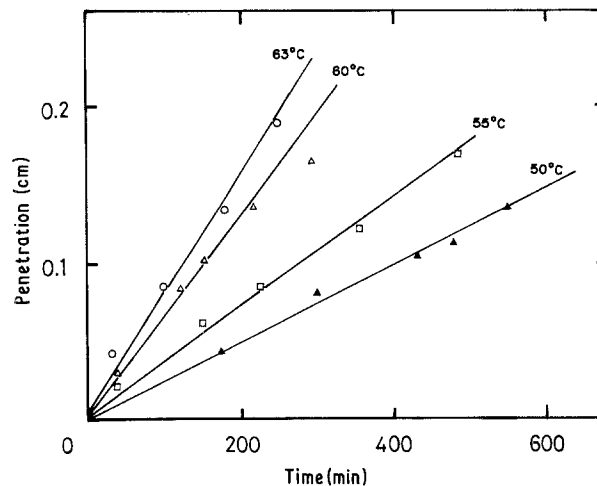


Figure 2 Penetration against time for methanol in PMMA.

azoisobisbutyronitrile (AIBN). 1 mg of AIBN was used for 1 ml of solution. Polymerization was conducted in a water bath at 40°C for 4 days and the sample obtained was annealed at 80°C for 4 days. Samples were cut and finally polished with 0.3 μm alumina. Details of the sample preparation are found elsewhere [9]. Sample dimensions were typically 19 mm \times 19 mm \times 5 mm.

The PMMA samples were immersed in ethanoic or methanoic Rh6G (5×10^{-5} M, Eastman Kodak, Laser grade). The temperature of the water bath was controlled within the accuracy of $\pm 0.5^\circ\text{C}$ during the diffusion process. Light with a wavelength of 530 nm was used for optical absorption measurements, since Rh6G/PMMA has an absorption maximum around 530 nm [8].

3. Results and discussion

3.1. PMMA immersed in ethanol and methanol solutions

A sharp boundary separating the swollen and unpenetrated region of PMMA is visually observed when a polymer sample is immersed in alcohol. It is said that surface compression in the swollen gel is balanced by biaxial tension in the unpenetrated core of the specimen and a steep stress gradient appears [3]. In Figs 1 and 2, the front penetration is seen to increase linearly with absorption time. Front penetration in the figures is represented by the distance from

the original position of the specimen surface to the front, and the penetration rate is the rate at which the front is moving into the glassy core. The distance from the surface of the swollen polymer to the advancing front, on the other hand, is relevant to the situation where the transport of the penetrant up to the front significantly controls overall kinetics. In addition, it is sensitive to the discontinuous reduction in the specimen thickness when the fronts meet [5].

An Arrhenius plot of $\ln(\text{penetration rate})$ as a function of $1/T$, (where T is absolute temperature) is shown in Figs 3 and 4. The activation energy of 23 kcal mol $^{-1}$ is obtained for both ethanol-PMMA and methanol-PMMA systems. Thomas and Windle [3] reported an activation energy of 27 kcal mol $^{-1}$ for the front penetration rate of the methanol-PMMA system at temperatures between 24 and 0°C. They also discussed that the value of the mentioned activation energy lay in the range of values reported for creep of glassy PMMA, i.e. 17–30 kcal mol $^{-1}$, and is far in excess of values appropriate to Fickian diffusion in glassy polymers, and that Case II diffusion could be described in terms of creep response of the polymer at the advancing front to the thermodynamic swelling stress.

The weight gain of the sample per unit area is plotted as a function of time (see Figs 5 and 6). For the ethanol-PMMA system in Fig. 5, there exists an "incubation period" at the lower temperatures of 45

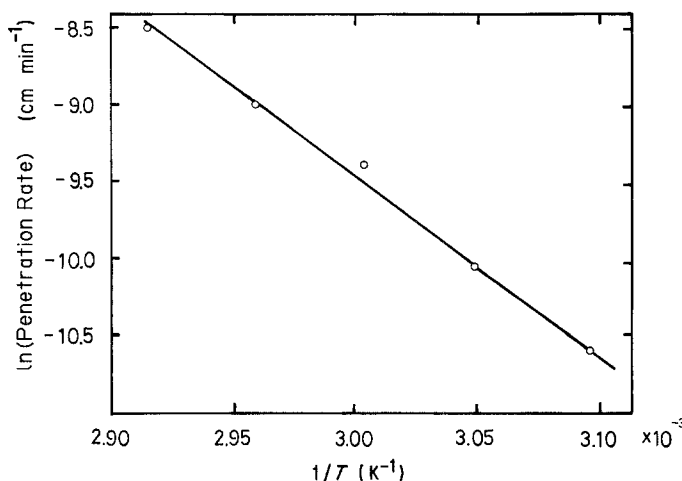


Figure 3 Arrhenius plot showing $\ln(\text{penetration rate})$ against $1/T$ for ethanol in PMMA.

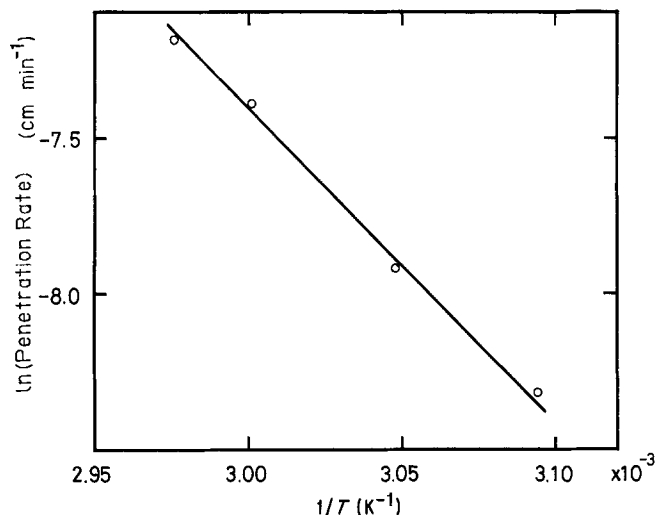


Figure 4 Arrhenius plot showing $\ln(\text{penetration rate})$ against $1/T$ for methanol in PMMA.

and 35°C before the sorption begins. A similar effect has been reported in the studies of Case II transport of n-propyl, i-propyl and n-butyl alcohol [3] and of methanol [5] diffusion in PMMA at ambient temperatures. The mentioned "incubation period" does not appear at elevated temperatures for the ethanol-PMMA system nor at temperatures between 50 and 63°C for methanol-PMMA. The "incubation period" is discussed in relation with the Case II viscous flow rate of the glass polymer in [10].

In Figs 5 and 6, the curves clearly display the characteristic sigmoidal shape. At lower temperatures, the absorption of both ethanol-PMMA and methanol-PMMA tends to follow Case II kinetics (weight gain/unit area, M_t , increases linearly with time, t), while at higher temperatures, departure from Case II kinetics becomes significant and the diffusion process becomes increasingly Fickian in character (M_t increases linearly with the square root of t).

Solution of Equation 1 with constant D , v and saturated surface concentration yields a plot of M_t against t sigmoidal in shape [11]. Based on the least square means fit, we approximated our experimental results to the solution of Equation 1 with D and v as parameters. Obtained values of D and v are listed in Tables IA and IB. As is reasonably expected, both D and v of ethanol-PMMA and methanol-PMMA

increase with temperature. The values of $D = 3.6 \times 10^{-8} \text{ cm}^2 \text{ sec}^{-1}$ and $v = 1.2 \times 10^{-6} \text{ cm sec}^{-1}$ at 50°C obtained by us for methanol-PMMA compare well with those of $D = 2.50 \times 10^{-8} \text{ cm}^2 \text{ sec}^{-1}$ and $v = 7.75 \times 10^{-7} \text{ cm sec}^{-1}$ at 42°C determined by Ware and Windle [11]. The above analysis may be a simplified one. Strain effects on the diffusion coefficients are taken into account in the more refined diffusion model in a manner consistent with the stress contribution to the flux [11].

3.2. PMMA immersed in ethanoic and methanoic Rh6G solutions

At first, dry PMMA was swollen to equilibrium in alcohol (ethanol or methanol), and then the swollen PMMA was immersed in alcoholic Rh6G solution. The well known Fickian diffusion relation describing M_t against t for a sample of thickness $2d$ and for small diffusion times is written as [12]

$$M_t/M_\infty = 2(D/\pi d^2)^{1/2} t^{1/2} \quad (2)$$

where M_∞ is weight gain/unit area at equilibrium. Optical density at 530 nm of Rh6G/PMMA is proportional to the amount of Rh6G in the sample, and Equation 2 becomes

$$(\text{OD})_t/(\text{OD})_\infty = 2(D/\pi d^2)^{1/2} t^{1/2} \quad (3)$$

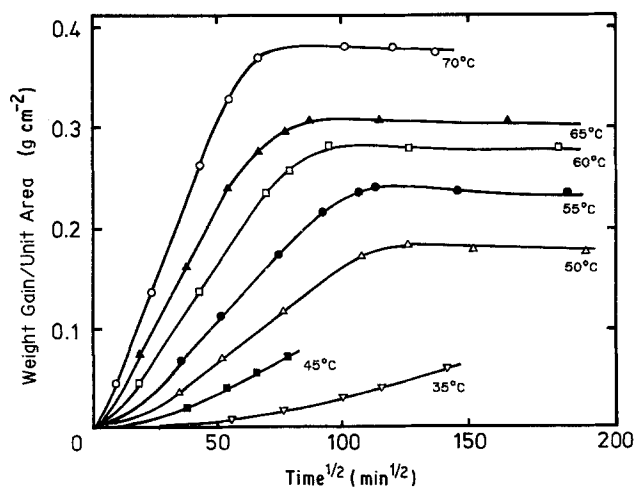


Figure 5 Weight gain/unit area against square root of time for ethanol in PMMA.

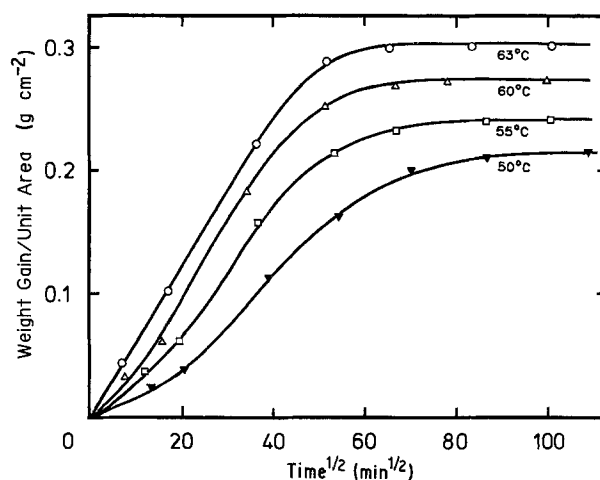


Figure 6 Weight gain/unit area against square root of time for methanol in PMMA.

TABLE IA Values of D and v obtained for ethanol-PMMA

	Temperature (°C)	50	55	60	65	70
Ethanol	D cm ² sec ⁻¹	1.0×10^{-8}	1.7×10^{-8}	3.2×10^{-8}	5.6×10^{-8}	8.8×10^{-8}
	v cm sec ⁻¹	3.3×10^{-7}	4.9×10^{-7}	6.6×10^{-7}	9.0×10^{-7}	1.3×10^{-6}

TABLE IB Values of D and v obtained for methanol-PMMA

	Temperature (°C)	50	55	60	63
Methanol	D cm ² sec ⁻¹	3.6×10^{-8}	7.9×10^{-8}	9.8×10^{-8}	1.5×10^{-7}
	v cm sec ⁻¹	1.2×10^{-6}	1.8×10^{-6}	2.1×10^{-6}	2.3×10^{-6}

in which $(OD)_t$ and $(OD)_\infty$ denote optical densities of the specimen at t and at equilibrium, respectively.

As is seen in Figs 7 and 8, Rh6G molecules are found to be introduced in the swollen PMMA followed by Fickian transport, which is reasonably expected since organic solvents in gel polymer diffuse by Fickian kinetics. Making use of Equation 2 and the results in Figs 7 and 8, we determined values of D at different temperatures for ethanoic Rh6G-PMMA and methanoic Rh6G-PMMA. The semi-log plots of $\ln D$ against $1/T$ are seen in Figs 9 and 10.

Generally the diffusion coefficient D is dependent on the concentration of the penetrant C , i.e. $D = D(C)$. Diffusion coefficient at zero penetrant concentration is written as

$$D(0) = D_0 \exp(-\Delta H_d/RT) \quad (4)$$

where D_0 is a constant; ΔH_d is the activation energy; R is the universal gas constant and T denotes absolute temperature. ΔH_d is constant in a relatively small temperature region.

In our experiments, Rh6G concentration is very low, i.e. 5×10^{-5} M, and the obtained D values may be approximated to $D(0)$. From Figs 9 and 10, ΔH_d of 41 kcal mol⁻¹ at temperatures between 55 and 70°C for ethanoic Rh6G-PMMA and that of 34 kcal mol⁻¹ between 55 and 63°C for methanoic Rh6G-PMMA were determined.

We then examined the transport of alcoholic Rh6G in a dry PMMA sample. A typical example of Rh6G optical density against immersion time for the dry and

the swollen PMMA sample is shown in Fig. 11. As mentioned already, diffusion of Rh6G in the swollen PMMA obeys Fickian kinetics, whereas, in the dry PMMA introduction of Rh6G molecules is very low before the advancing fronts meet (indicated by arrow in the figure), after which the transport behaviour is similar to that in the initially swollen sample. Similar results are obtained for other ethanoic and methanoic Rh6G-PMMA systems at different temperatures.

During the sorption process, internal stresses exist in the swollen glassy region of the polymer and are thought to contribute significantly to the anomalous diffusion observed in many penetrant-polymer systems such as methanol-PMMA [11]. Introduction of Rh6G-alcohol in dry PMMA is thought to be greatly hindered before the advancing fronts meet owing to the internal stresses. Unfortunately, optical density results before the advancing fronts have met are very difficult to analyse the transport behaviour of Rh6G quantitatively. Diffusion equations of the three component systems with interacting flows have been solved in which the cross-term diffusion coefficients as well as main diffusion coefficients were taken into account [13]. In our experiments, addition of Rh6G is seen to bring no change on the sorption behaviour of alcohol in PMMA.

The front surface of a PMMA sample immersed in alcoholic Rh6G solution is successively polished and optical absorption of the sample at 530 nm is measured to determine the concentration profile of Rh6G

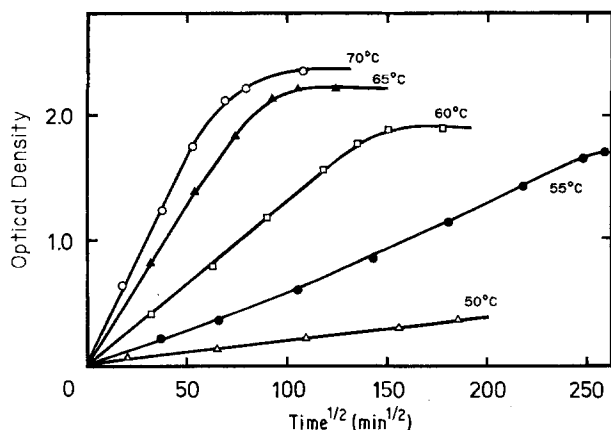


Figure 7 Optical density against square root of time for Rh6G in swollen PMMA with equilibrium ethanol.

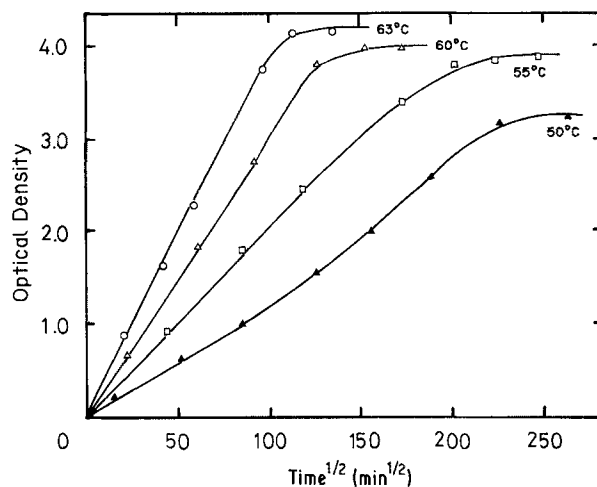


Figure 8 Optical density against square root of time for Rh6G in swollen PMMA with equilibrium methanol.

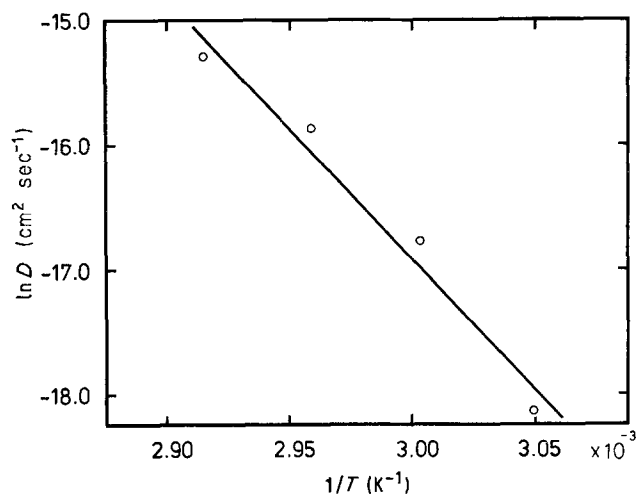


Figure 9 $\ln D$ (diffusion coefficient) against $1/T$ for Rh6G in PMMA swollen to equilibrium with ethanol.

in the specimen. The sharp reduction of Rh6G concentration at the front, peculiar to Case II kinetics, is not observed in our investigations. Almost all the Rh6G molecules are distributed within 0.25 mm from the surface for the PMMA sample immersed in ethanoic Rh6G at 60°C for 1770 min; while the penetrating front exists at about 1.75 mm from the surface. Iodine in methanol is found to follow methanol for the PMMA-methanol/iodine system [5], while Rh6G molecules penetrate in PMMA behind the alcohol.

Rh6G molecules in ethanol become monomeric, i.e. the Rh6G absorption spectra are concentration independent, at concentrations below 1.65×10^{-4} M and at temperatures above -78.5°C [14]. Rh6G (colour index 45160) is a phenyl-xanthene derivative and may stretch longer than 1 nm in length. The π -electron distribution of Rh6G is described in terms of two identical mesomeric structures where π -electrons oscillate between end amino groups of the dye. Maximum absorption of Rh6G is solvent dependent, since the amino groups of the dye are not fully alkylized [15]. In ethanol, Rh6G shows an absorption maximum at 530 nm, while in isopropylalcohol, at 514 nm.

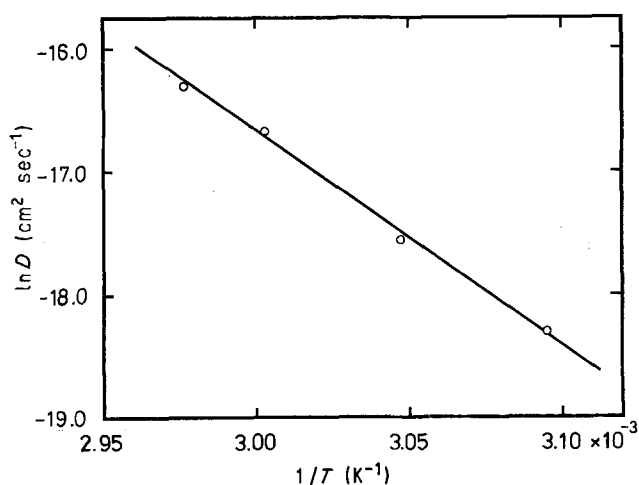


Figure 10 $\ln D$ (diffusion coefficient) against $1/T$ for Rh6G in PMMA swollen to equilibrium with methanol.

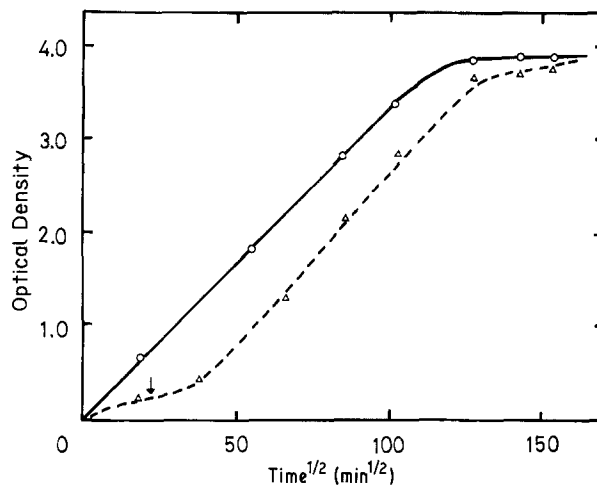


Figure 11 Optical density against square root of time for methanoic Rh6G-PMMA system at 60°C. White circles show the results for Rh6G diffusion in PMMA swollen to equilibrium with methanol and white triangles, in dry PMMA. The arrow in the figure indicates the time when the fronts met.

As described previously, diffusion of Rh6G in rubbery alcoholic PMMA follows Fickian transport and the diffusion coefficient of Rh6G dye is quantitatively determined. The front penetration rate is faster in the methanol-PMMA rather than in the ethanol-PMMA system, and furthermore, equilibrium concentration of Rh6G in PMMA, determined from optical density measurements, is about twice as large for methanoic Rh6G-PMMA system as for ethanoic Rh6G-PMMA.

Acknowledgements

Authors wish to express their thanks to Mr S. Takeuchi for his assistance of the present work.

References

1. H. L. FRISCH, T. T. WANG and T. K. KWEI, *J. Polym. Sci. A-2* **7** (1969) 879.
2. T. T. WANG, T. K. KWEI and H. L. FRISCH, *ibid.* **7** (1969) 2019.
3. N. L. THOMAS and A. H. WINDLE, *Polymer* **21** (1980) 613.
4. T. K. KWEI, T. T. WANG and H. M. ZUPKO, *Macromolecules* **5** (1972) 645.
5. N. L. THOMAS and A. H. WINDLE, *Polymer* **19** (1978) 255.
6. N. L. THOMAS and A. H. WINDLE, *ibid.* **22** (1981) 627.
7. O. G. PETERSON and B. B. SNAVELY, *Appl. Phys. Lett.* **10** (1967) 208.
8. J. MUTO and K. KOBAYASHI, *Phys. Status Solidi (a)* **84** (1984) k29.
9. F. HIGUCHI and J. MUTO, *Phys. Lett.* **A99** (1983) 121.
10. N. L. THOMAS and A. H. WINDLE, *Polymer* **23** (1982) 529.
11. R. H. WARE and A. H. WINDLE, *J. Appl. Polym. Sci.* **25** (1980) 717.
12. J. CRANK, in "Mathematics of Diffusion" (Oxford University Press, London, 1967) Ch. 4.
13. H. FUJITA, *J. Phys. Chem.* **63** (1959) 242.
14. J. E. SELWYN and J. H. STEINFELD, *ibid.* **76** (1972) 762.
15. K. H. DREXHAGE, in "Structures and Properties of Laser Dyes" edited by E. P. Schaefer (Springer-Verlag, Berlin, 1973) Ch. 4.

Received 13 May

and accepted 14 August 1985